FISEVIER

Contents lists available at ScienceDirect

Fish and Shellfish Immunology

journal homepage: www.elsevier.com/locate/fsi



Full length article

STAT2 negatively regulates RIG-I in the antiviral innate immunity of black carp

Ji Liu ^{a,b,1}, Chushan Dai ^{a,1}, Lijun Yin ^a, Xiao Yang ^a, Jun Yan ^a, Meiling Liu ^b, Hui Wu ^a, Jun Xiao ^a, Weiguang Kong ^c, Zhen Xu ^c, Hao Feng ^{a,*}

- a State Key Laboratory of Developmental Biology of Freshwater Fish, College of Life Science, Hunan Normal University, Changsha, 410081, China
- ^b College of Chemistry and Chemical Engineering, Hunan Normal University, Changsha, 410081, China
- ^c State Key Laboratory of Freshwater Ecology and Biotechnology, Institute of Hydrobiology, Chinese Academy of Sciences, Wuhan, 430072, China

ARTICLE INFO

Keywords: Innate immunity RIG-I STAT2 Black carp

ABSTRACT

The signal transducer and activator of transcription 2 (STAT2), a downstream factor of type I interferons (IFNs), is a key component of the cellular antiviral immunity response. However, the role of STAT2 in the upstream of IFN signaling, such as the regulation of pattern recognition receptors (PRRs), remains unknown. In this study, STAT2 homologue of black carp (Mylopharyngodon piceus) has been cloned and characterized. The open reading frame (ORF) of bcSTAT2 comprises 2523 nucleotides and encodes 841 amino acids, which presents the conserved structure to that of mammalian STAT2. The dual-luciferase reporter assay and the plaque assay showed that bcSTAT2 possessed certain IFN-inducing ability and antiviral ability against both spring viremia of carp virus (SVCV) and grass carp reovirus (GCRV). Interestingly, we detected the association between bcSTAT2 and bcRIG-I through co-immunoprecipitation (co-IP) assay. Moreover, when bcSTAT2 was co-expressed with bcRIG-I, bcSTAT2 obviously suppressed bcRIG-I-induced IFN expression and antiviral activity. The subsequent co-IP assay and immunoblotting (IB) assay further demonstrated that bcSTAT2 inhibited K63-linked polyubiquitination but not K48-linked polyubiquitination of bcRIG-I, however, did not affect the oligomerization of bcRIG-I. Thus, our data conclude that black carp STAT2 negatively regulates RIG-I through attenuates its K63-linked ubiquitination, which sheds a new light on the regulation of the antiviral innate immunity cascade in vertebrates.

1. Introduction

Type I interferons (IFNs) act as highly important antiviral cytokines in vertebrates [1,2]. Upon virus infection, pattern recognition receptors (PRRs), such as RIG-I-like receptors (RLRs), recognize pathogen-associated molecular patterns (PAMPs) and activate downstream signaling molecules to induce the production of type I IFNs [3–5]. Secreted IFNs bind to the interferon- α/β receptor (IFNAR) of neighbor cells, which in turn activates the downstream Janus kinase–signal transducer and activator of transcription (JAK-STAT) signaling pathway and ultimately triggers the expression of interferon-stimulated genes (ISGs), most of which are antiviral proteins and pro-inflammatory cytokines [6–8].

In mammals, STAT family consists of seven members, including

STAT1, STAT2, STAT3, STAT4, STAT5a, STAT5b and STAT6, which share a N-terminal domain (ND), a coiled-coil domain (CCD), a DNA-binding domain (DBD), a linker domain (LD), a Src homology 2 domain (SH2), and a transactivation domain (TAD) [9,10]. Type I IFNs induced by viral infection interact with their cognate IFNARs, promoting STAT1, STAT2 and IRF9 to form interferon-stimulated gene factor 3 (ISGF3) complex, which enters the nucleus and binds to IFN-stimulated response element (ISRE) of ISGs to initiate ISGs transcription, resulting in a cellular antiviral state [8,11]. Human ($Homo\ sapiens$) STAT1 (HsSTAT1), named HsSTAT1a and HsSTAT1β, was reporter for the first time in 1990 [12]. However, HsSTAT1a but not HsSTAT1β contains a complete TAD domain [13]. Similarly, HsSTAT2 contains the corresponding six domains. STAT1 and STAT2 play an important role in the antiviral immunity. STAT1-deficient mice are more susceptible to

^{*} Corresponding author. State Key Laboratory of Developmental Biology of Freshwater Fish, College of Life Science, Hunan Normal University, Changsha, Hunan, 410081, China.

E-mail address: fenghao@hunnu.edu.cn (H. Feng).

 $^{^{1}\,}$ These authors contributed equally to this paper.

Table 1
Primers used in the study.

Primer name	Sequence (5'-3')	Primer information
bcSTAT2-F	ACTGACGGTACCGCCACCATGACTCAGTGGGAG	ORF cloning
bcSTAT2-R	ACTGACCTCGAGGGGGTCAGCGGCA	
bcSTAT2-△N–F	ACTGACGGTACCGCCACCGCACAGCAAGTGCAG	Mutant construction
bcSTAT2-△CC-F1	ACTGACGGTACCGCCACCGCAGAGCTTTGTAGAGACTC	
bcSTAT2-△CC-R1	ACTGACCTCGAGAGTCTCTACAAGCTCTGCATCAT	
bcSTAT2-△DBD-F1	ACTGACGGTACCGCCACCTCATTTGTTCTTCCAGCCTCCTGGG	
bcSTAT2-△DBD-R1	ACTGACCTCGAGGGCTGGAAGAACAAATGAGCTC	
bcSTAT2-△LD-F1	ACTGACGGTACCGCCACCGAAAGCCCTAGCTACTTGTCAGAC	
bcSTAT2-△LD-R1	ACTGACCTCGAGCAAGTAGCTAGGGCTTTCAAAA	
bcSTAT2-△SH2–F1	ACTGACGGTACCGCCACCCTGGTTAAAGGCAAATACTACAG	
bcSTAT2-△SH2-R1	ACTGACCTCGAGGTATTTGCCTTTAACCAGGG	
bcSTAT2-△TAD-R1	ACTGACCTCGAGAAAGGCCTGGTCTTTAG	
bcactin-Q-F	TGGGCACCGCTGCTTCCT	ex vivo q-PCR
bcactin-Q-R	TGTCCGTCAGGCAGCTCAT	
bcSTAT2-Q-F	GGAGAATCTGGACAACC	
bcSTAT2-Q-R	ATCCTGCTGCTCCTCC	
SVCV-G-Q-F	GATGACTGGGAGTTAGATGGC	
SVCV-G-Q-R	ATGAGGGATAATATCGGCTTG	
SVCV-P-Q-F	AACAGGTATCGACTATGGAAGAGC	
SVCV-P-Q-R	GATTCCTCTTCCCAATTGACTGTC	
SVCV-M-Q-F	CGACCGCGCCAGTATTGATGGATAC	
SVCV-M-Q-R	ACAAGGCCGACCCGTCAACAGAG	

bacteria and virus infection [14–16]. Meanwhile, STAT2 deficiency in mice are also sensitive to virus infection and increases the replication of vesicular stomatitis virus (VSV) and dengue virus [17,18]. Moreover, the role of STAT2 in antiviral signaling is further supported by a study in which child lacking STAT2, caused by a homologous mutation in intron 4, has a history of disseminated vaccine-strain measles [19]. In addition, studies have reported that STAT2 has the tumor suppression activity and participates in antitumor immunity [20,21]. In teleost, STAT2 has been cloned and characterized from some species, such as orange-spotted grouper (*Epinephelus coioides*) [22], turbot (*Scophthalmus maximus*) [23], rock bream (*Oplegnathus fasciatus*) [24]. However, there have been few studies on the role of STAT family in regulating PRRs, such as RIG-I. So far, researchers have only found that STAT4 binds to E3 ligase CHIP, preventing CHIP-mediated proteasomal degradation of RIG-I by K48-linked ubiquitination [25].

RIG-I is the key sensor to recognize cytosolic RNA components of invading microorganisms and induces the production of type I IFNs and inflammatory cytokines [26,27]. The deficiency of RIG-I dampens host innate immunity against viruses and bacteria; however, the over-activation of RIG-I leads to the development of autoimmune diseases. Therefore, the activation of RIG-I is strictly regulated to moderate type I IFNs production and to maintain the host immune homeostasis. Interacting protein is one of an important mean to regulate the activity of RIG-I. In mammals, the double-stranded RNA-binding protein PACT interacts with C-terminal RD domain of RIG-I and increases RIG-I-induced type I IFNs expression [28]. In addition, NDR2 stabilizes the interaction between RIG-I and TRIM25, promoting TRIM25-induced K63-linked ubiquitination of RIG-I [29]. On the contrary, the pyrin-containing NLR members, NLRP12 binds to TRIM25, blocking its ability to ubiquitylate and activate RIG-I [30]. In teleost, bcLGP2 interacts with bcRIG-I and enhances the K48-linked ubiquitination of bcRIG-I, thereby resulting in the degradation of bcRIG-I [31]. Meanwhile, grass carp LGP2 restrained the K63-linked ubiquitination of grass carp RIG-I [32].

Our previous study has reported that bcRIG-I presented strong antiviral activity against GCRV and SVCV [33]. Moreover, STAT1 homologues of black carp, named as bcSTAT1a and bcSTAT1b, has been also cloned and characterized in our lab [34]. In this study, we have cloned bcSTAT2 and identified that bcSTAT2 expression alone had certain IFN-inducing ability and antiviral activity. However, when co-expressed with bcRIG-I, bcSTAT2 attenuated the K63-linked ubiquitination of bcRIG-I, thereby inhibiting bcRIG-I-induced IFN expression

and antiviral activity. These data will elucidate a new regulatory mechanism of RLR/IFN signaling pathway in vertebrates and provide a new idea for studying the mechanism of antiviral innate immune in other vertebrates and even humans.

2. Materials and methods

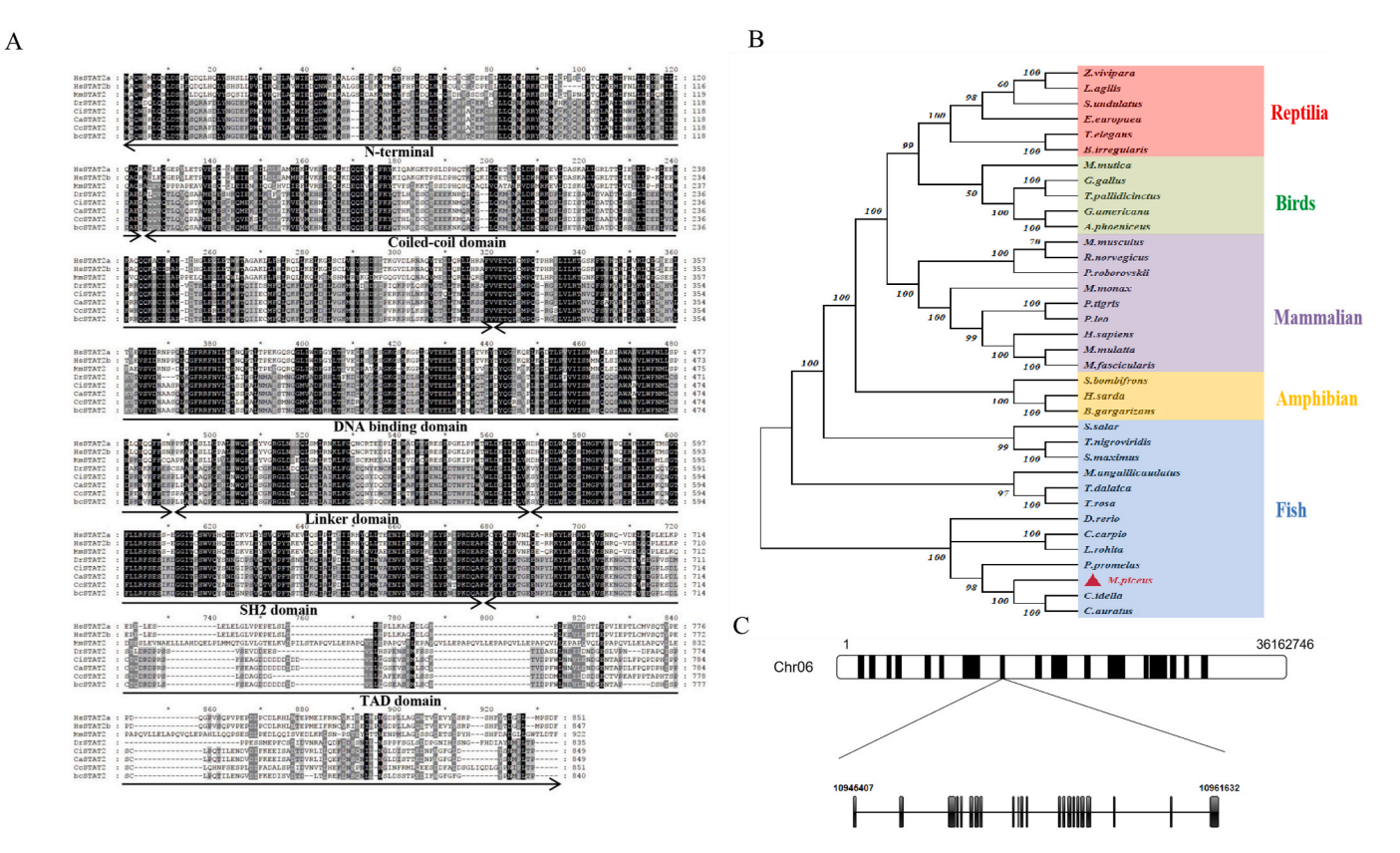
2.1. Cells and plasmids

Epithelioma papulosum cyprini (EPC), Ctenopharyngodon idella kidney (CIK), Mylopharyngodon piceus kidney (MPK) and Human embryonic kidney 293T (HEK293T) cells were kept in our lab. All cell lines were maintained in Dulbecco's modified Eagle's medium (DMEM) supplemented with 10% fetal bovine serum, 2 mM L-glutamine, 100 u/ml penicillin and 100 mg/ml streptomycin. EPC, CIK and MPK cells were cultured at 28 °C with 5% CO2, however, HEK293T cells were cultured at 37 °C with 5% CO2.

pcDNA5/FRT/TO-HA-Ub and pRL-TK were kind gifts from Dr. Pinghui Feng (University of Southern California, USA). pcDNA5/FRT/ TO (Invitrogen, USA), pcDNA5/FRT/TO-HA-K63O-Ub, pcDNA5/FRT/ TO-HA-K48O-Ub, Luci-bcIFNa (for black carp IFNa promoter activity analysis), Luci-eIFN (for EPC IFN promoter activity analysis), Luci-hISRE (for human IFN-stimulated response element promoter activity analysis) and Luci-DrIFN ϕ 3 (for zebrafish IFN ϕ 3 promoter activity analysis) were kept in our lab. The plasmid expressing bcRIG-I was constructed in our previous study [33]. The open reading frame (ORF) of bcSTAT2 was cloned from MPK cells and inserted into pcDNA5/FRT/To with a HA tag or a Myc tag at the C-terminus separately. The recombinant expression vectors pcDNA5/FRT/TO/-bcSTAT2-\(\triangle ND-Myc\), pcDNA5/FRT/TO/bcSTAT2-∕\CCD-Mvc, pcDNA5/FRT/TO/-bcSTAT2-\DBD-Myc, pcDNA5/FRT/TO/-bcSTAT2-\LD-Myc, pcDNA5/FRT/TO/- bcSTAT2-\SH2-Myc and pcDNA5/FRT/TO/-bcSTAT2-\\TAD-Myc were constructed by cloning the predicted functional domain of bcSTAT2 into pcDNA5/FRT/TO-Myc (C). All primers' information was listed in Table 1.

2.2. Virus production and antiviral assay

GCRV (strain: GCRV873) and SVCV (strain: SVCV741) were kept in our lab, which were propagated in CIK and EPC cells in the presence of 2% FBS at 28 °C, respectively. The viral titer was measured by the plaque assay as previously [31]. EPC cells in 24-well plate were



 $\textbf{Fig. 1.} \ \ \textbf{Sequence analysis of bcSTAT2}$

(A) Amino acid sequence alignment of bcSTAT2 with other vertebrate STAT2 homologues, including *H.sapiens* 2a (AAA98760.1), *H. sapiens* 2b (NP_938146.1), *M. musculus* (NP_064347.1), *D. rerio* (NP_001258730.1), *C. idella* (AMB20880.1), *C. auratus* (AFL69829.1), *C. carpio* (AJP77392.1), *M. piceus* (AZP56657.1), by using MEGA 6.0 program and GENEDOC. The protein domains were predicted by CDS (Conserved Domain Search) of NCBI (http://www.ncbi.nlm.nih.gov/structure/cdd/wrpsb.cgi). (B) The phylogenetic tree of STAT2 from different species were constructed by MEGA6.0 program, which are same to those in Table 2. (C) The genomic information of bcSTAT2. The chromosome analysis map is done using the online tool IBS (http://ibs.biocuckoo.org/online.php#).

transfected with the plasmids expressing bcSTAT2 or the empty vector, and infected with SVCV (MOI = 0.001, 0.01) or GCRV (MOI = 0.01, 0.1) at 24 h post transfection (hpt). 24 h after infection, the corresponding cell supernatant was collected and frozen at $-80\,^{\circ}\text{C}$. The corresponding viral supernatant was added into EPC cells in the 24-well plate by 10-fold dilution method $(10^{-1}{\sim}10^{-7})$ and incubated for 2 h at 28 $^{\circ}\text{C}$. The supernatant was replaced with fresh DMEM containing 2% FBS and 0.75% methylcellulose (Sangon, China) after incubation. When cells showed obvious CPE phenomenon (generally 72 h–96 h), crystal violet staining was performed to calculate the number of viral spots in each pore.

2.3. Poly (I:C), GCRV and SVCV treatment

MPK cells were seeded in 6-well plate (1 \times 10 6 cells/well) 24 h before treatment. Poly (I:C) (Sigma, USA) was used for synthetic dsRNA stimulation, which was heated to 55 °C (in PBS) for 5 min and cooled at room temperature before use. MPK cells were replaced with fresh media containing Poly (I:C) at different concentrations (5 $\mu g/ml$, 25 $\mu g/ml$ or 50 $\mu g/ml$) and harvested at different time points post treatment separately. For GCRV and SVCV infection, MPK cells in 6-well plate (1 \times 10 6 cells/well) were treated with GCRV or SVCV at different MOI (0.01,0.1,1) separately and harvested at different time points post infection.

2.4. RNA extraction and quantitative real-time PCR (qRT-PCR)

Total RNA from treated EPC or MPK cells in 6-well plate was extracted using the RNA rapid extraction kit (Magen, China). The RNA

was reverse-transcribed using reverse transcriptase (Takara, Japan). The relative transcription level of bcSTAT2 and SVCV-M (P, G) was tested through qRT-PCR by using Applied Biosystems QuantStudio 5 Real Time PCR Systems (Thermo Fisher, USA). The qRT-PCR program was: 1 cycle of 95 °C/10 min, 40 cycles of 95 °C/15 s, 60 °C/1 min. The $2^{-\Delta\Delta CT}$ method was applied to calculate the relative expression difference of target genes, and data were normalized by β -actin expression as the internal control.

2.5. Immunoblotting (IB)

HEK293T cells and EPC cells in 6-well plate were transfected with the indicated plasmids respectively. The transfected cells were harvested at 48 hpt and boiled for IB assay as previously [31]. In brief, the target protein was separated by 8% SDS-PAGE and then transferred to PVDF membrane. Afterward, the membrane was probed with mouse anti-Myc monoclonal antibody (Abmart), followed by the incubation with the secondary antibody (Sigma). Finally, the target proteins were detected by NBT/BCIP alkaline phosphatase substrate (Thermo Fisher).

2.6. Co-immunoprecipitation (Co-IP)

HEK293T cells in 100 mm were co-transfected with plasmids expressing bcSTAT2 and/or bcRIG-I, and collected for co-IP assay at 48 hpt. The transfected cells were lysed with 1% NP-40 lysis buffer containing protease inhibitor cocktails. After centrifugation, the cell debris was discarded and the supernatant was incubated with protein A/G agarose beads at 4 $^{\circ}$ C for 1 h. Anti-Flag-conjugated (or anti-HAconjugated) agarose beads were incubated with the supernatant at

Table 2
Comparison of bcSTAT2 with other vertebrate STAT2 (%).

Species	GenBank accession number	Full-length sequence	
		Identity	Similarity
Mylopharyngodon piceus	AZP56657.1	100%	100%
Carassius auratus	AFL69829.1	94.9%	96.2%
Ctenopharyngodon idella	AMB20880.1	94.8%	96.3%
Pimephales promelas	XP_039545086.1	86.4%	90.5%
Cyprinus carpio	AJP77392.1	81.7%	88.2%
Labeo rohita	XP_050967968.1	79.5%	85.8%
Danio rerio	NP_001258730.1	79.2%	87.8%
Triplophysa dalaica	XP_056605751.1	70.3%	81.2%
Triplophysa rosa	KAI7807479.1	79.0%	88.2%
Misgurnus anguillicaudatus	XP_055068931.1	70.0%	81.0%
Salmo salar	NP_001138896.1	63.1%	76.5%
Scophthalmus maximus	ACX69848.1	58.6%	74.2%
Tetraodon nigroviridis	AFQ98274.1	57.0%	73.0%
Mauremys mutica	XP_044851387.1	46.4%	65.9%
Spea bombifrons	XP_053311646.1	47.5%	63.9%
Euleptes europaea	XP_056711592.1	43.5%	65.2%
Thamnophis elegans	XP_032064703.1	42.0%	62.2%
Bufo gargarizans	XP_044140748.1	45.0%	64.1%
Agelaius phoeniceus	XP_054505189.1	41.8%	61.5%
Hyla sarda	XP_056418350.1	44.1%	62.7%
Sceloporus undulatus	XP_042305569.1	42.6%	62.1%
Zootoca vivipara	XP_034959598.1	42.5%	62.4%
Lacerta agilis	XP_032994520.1	41.4%	61.9%
Tympanuchus pallidicinctus	XP_052521163.1	41.5%	62.3%
Rattus norvegicus	NP_001011905.1	42.5%	61.3%
G.gallus	XP_015155768.1	41.2%	62.1%
Panthera leo	XP_042802806.1	42.4%	60.7%
Panthera tigris	XP_007081564.2	42.4%	60.6%
Grus americana	XP_054663250.1	41.5%	62.3%
Macaca fascicularis	XP_005571290.1	43.1%	61.9%
Macaca mulatta	NP_001253856.1	43.1%	64.4%
Homo sapiens	NP_005410.1	42.8%	62.2%
Mus musculus	NP_064347.1	41.9%	61.4%
Phodopus roborovski	XP_051032028.1	41.8%	61.5%
Sus scrofa	NP_999054.1	40.1%	57.0%
Marmota monax	XP 046322667.1	41.8%	63.1%

4 °C for 4 h. After 4 times of wash with 1%NP-40 buffer, the Flag peptide (HA peptide) was used to elute the proteins bound to the agarose beads. Finally, the proteins were boiled in 5 \times sample buffer and applied to IB assay as above.

2.7. Immunofluorescence microscopy

The transfected cells in 24-well plate were treated with 4% (v/v)

В

paraformaldehyde at 24 hpt, permeabilized with Triton X-100 (0.2% in PBS) and then applied for immunofluorescent (IF) staining as previously described [34]. Rabbit monoclonal anti-HA antibody was probed at the ratio of 1:500 (Sigma), accordingly, Alexa 594-conjugated secondary antibody was probed at the ratio of 1:1000 (Sigma); DAPI was applied to nucleus staining.

2.8. Dual-luciferase reporter assay

EPC cells seeded in 24-well plate were transfected with the indicated plasmids in figures. For each transfection, the total amount of plasmid was balanced with the empty vector. The cells were harvested at 24 hpt and lysed by PLB buffer for 15 min on ice. The supernatant was used to measure the activities of firefly luciferase and renilla luciferase by dual-Luciferase reporter assay system (Promega).

2.9. Semi-denaturing detergent agarose gel electrophoresis (SDD-AGE)

The transfected HEK293T cells in 100 mm were harvested at 48 hpt and then treated with 1%NP-40 lysis buffer. After centrifugation, the supernatant was mixed with 5 \times loading buffer. The horizontal 1.5% agarose gel made with 1 \times TBE and 0.1% SDS was used to divide the samples at 100 V for 80 min at 4 $^{\circ}$ C [35]. Eventually, the proteins were transferred to PVDF membrane for IB assay as above.

2.10. Statistics analysis

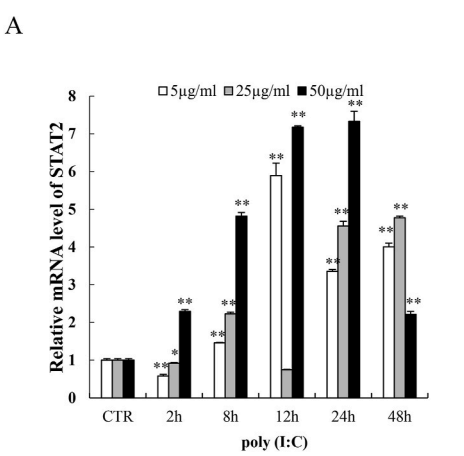
All data of qRT-PCR, dual-luciferase reporter assay and viral titration, were acquired from the average values of three independent experiments, and each experiment was repeated with three times. The student's t-test indicates the statistical significance between the groups. Asterisk * stands for p<0.05, which means statistically significant; ** stands for p<0.01 which means the high significance of statistic.

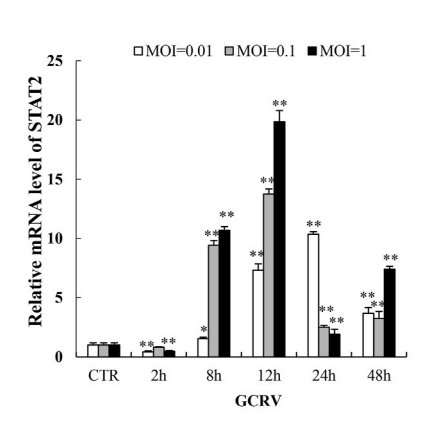
3. Results

3.1. Molecular cloning and sequence analysis of bcSTAT2

C

To explore the role of STAT2 in black carp innate immunity, the full-length cDNA of bcSTAT2 was cloned and identified from MPK cells (Fig. S1). The CDS of bcSTAT2 (NCBI accession number: MH410169.1) consists of 2523 nucleotides and encodes 841 amino acids, which contains ND, CCD, DBD, LD, SH2 and TAD (Fig. 1A). To investigate the conservation of STAT2 in vertebrate, the amino acid sequence of





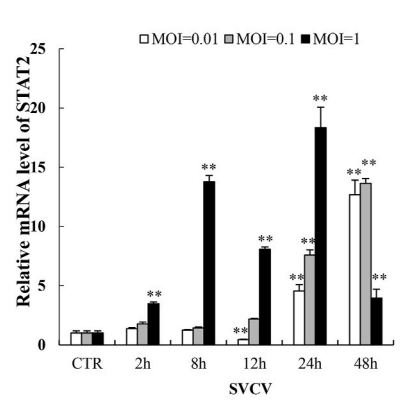


Fig. 2. The mRNA level of bcSTAT2 under various stimulation

MPK cells in 6-well plate (1 \times 10⁶ cells/well) were treated with poly (I:C) (A) at indicated concentrations, or infected with GCRV (B) or SVCV (C) at different MOI respectively. The cells were harvested at indicated time points post stimulation for qRT-PCR to detect the mRNA level of bcSTAT2. The asterisk (* or **) indicated the fold changes are significant different compared with the control. *p < 0.05, **p < 0.01.

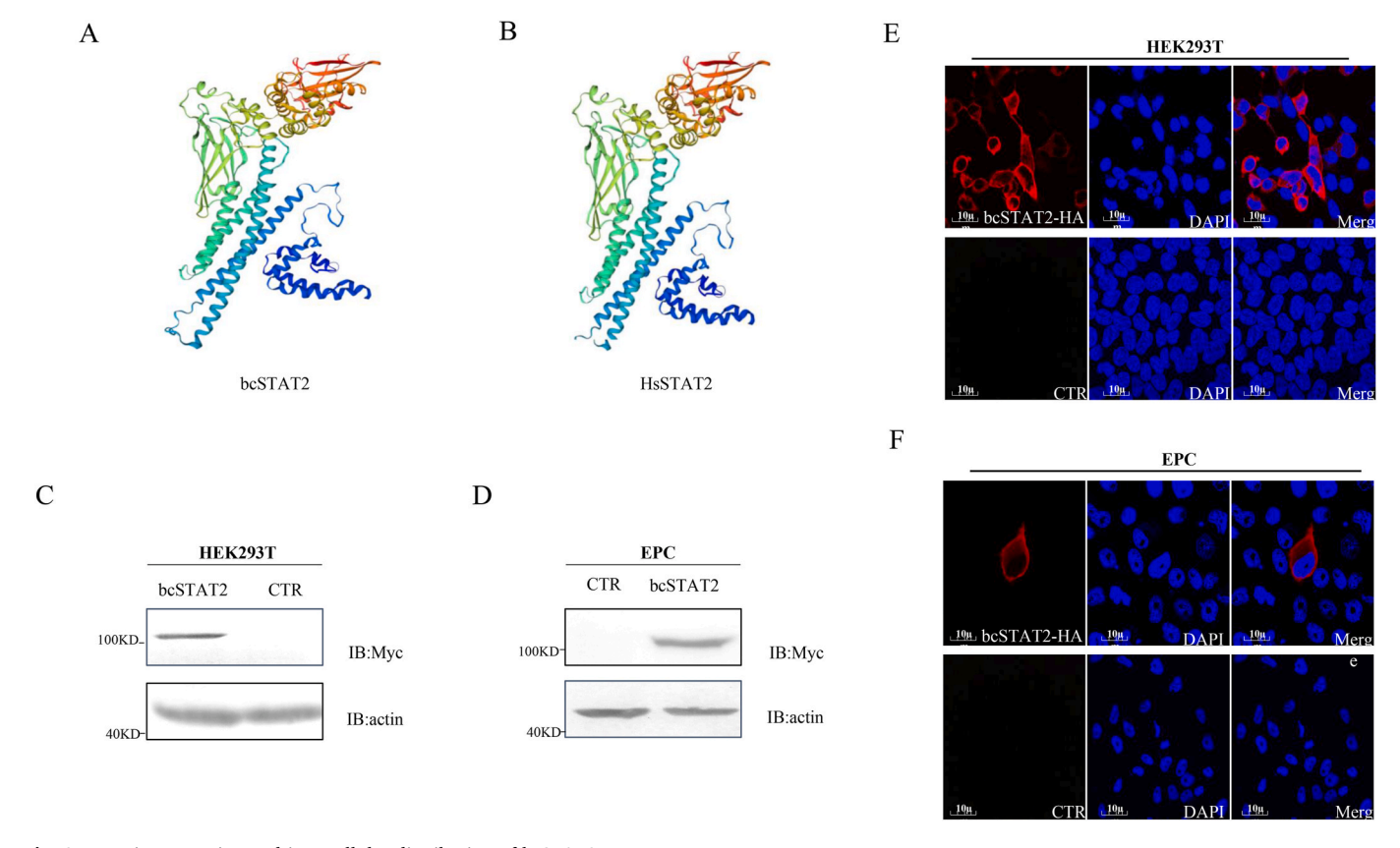


Fig. 3. Protein expression and intracellular distribution of bcSTAT2 (A–B) The predicted three-dimensional structures of bcSTAT2 and human STAT2 (HsSTAT2) were constructed by the online program SWISS-MODEL. HEK293T cells (C) and EPC cells (D) in 6-well plate (2×10^6 cells/well) were transfected with plasmids expressing bcSTAT2 or the empty vector (3 μ g) respectively. The IB assay was used to detect the expression of the bcSTAT2 protein. (E–F): HEK293T cells (E) and EPC cells (F) in 24-well plate (5×10^4 cells/well) were transfected with bcSTAT2 (400 ng) respectively, and applied to the IF staining at 24 hpt. CTR: pcDNA5/FRT/TO; bcSTAT2: pcDNA5/FRT/TO-bcSTAT2-Myc; bcSTAT2-HA: pcDNA5/FRT/TO-bcSTAT2-HA.

bcSTAT2 has been subjected to diverse alignment with those of STAT2 proteins from different species, including human, mouse (*Mus musculus*), zebrafish (*Danio rerio*), grass carp (*Ctenopharyngodon idella*), crucian carp (*Carassius auratus*) and common carp (*Cyprinus carpio*). The result revealed that STAT2 is a conserved protein among vertebrates (Fig. 1A). Phylogenetic analysis was applied to bcSTAT2 and STAT2 proteins of other species, which was conducted by using the maximum likelihood method with 500 replications of bootstrap. The result shows that bcSTAT2 shares the highest similarity with grass carp STAT2 (96.3%) and crucian carp STAT2 (96.2%) (Fig. 1B and Table 2). Based on the genome information of black carp, we found that *bcSTAT2* gene is located on chromosome 6 and is composed of 22 exons (Fig. 1C).

3.2. bcSTAT2 transcription in response to various stimulation

To learn the expression of bcSTAT2 during the innate immune activation, MPK cells were subjected to different stimuli, including poly (I: C), GCRV and SVCV, and the mRNA level of bcSTAT2 was examined by qRT-PCR. In the poly (I:C) treated MPK cells, the mRNA level of bcSTAT2 was slightly increased in all groups, except that of 12 h point in 25 $\mu g/ml$ group. The highest mRNA level of bcSTAT2 (24 h, 50 $\mu g/ml)$ within 48 h post stimulation was up to 7.3-fold of that of the control (Fig. 2A). In GCRV infected MPK cells, the mRNA level of bcSTAT2 was decreased at 2 h post infection (hpi) and then enhanced at 8 hpi in all groups. The highest level of bcSTAT2 was up to 19.8-fold at 12 hpi in 1 MOI group of that of the control (Fig. 2B). In SVCV infected MPK cells, the mRNA level of bcSTAT2 did not significantly change in the early stage of SVCV infection, but was obviously improved at 24 hpi and reached the peak at 48 hpi in 0.01 and 0.1 MOI group. However, the

mRNA level of bcSTAT2 was quickly increased and reached a maximum at 24 hpi in 1 MOI group (Fig. 2C). In general, these data implied that bcSTAT2 was involved in host innate immune response initiated by GCRV and SVCV.

3.3. Protein expression and subcellular distribution of bcSTAT2

To investigate the function of bcSTAT2, the protein structure of bcSTAT2 and human STAT2 (HsSTAT2) was predicted by the Swiss Model (https://swissmodel.expasy.org/). Fig. 3A and B shows that the protein structure of bcSTAT2 is highly similar to that of HsSTAT2, implying the functional conservation between bcSTAT2 and HsSTAT2. HEK293T cells and EPC cells were transfected with the plasmid expressing bcSTAT2 or the empty vector independently, and harvested for IB assay at 48 hpt. The specific band of $\sim\!106\,\mathrm{kDa}$ was detected in the cell lysates of both HEK293T and EPC cells transfected with bcSTAT2 but not the empty vector (Fig. 3C&D). The results demonstrated that bcSTAT2 was well expressed in both mammalian and fish cells.

To determine the subcellular distribution of bcSTAT2. Both HEK293T cells and EPC cells were transfected with the plasmid expressing bcSTAT2 or the empty vector respectively, and used for the IF staining assay. In the data of IF, the brilliant red color representing bcSTAT2-expressing area was detected in cytoplasm of HEK293T and EPC cells (Fig. 3E&F). The results demonstrated that bcSTAT2 was mainly distributed in the cytoplasm.

3.4. The IFN-inducing activity and antiviral ability of bcSTAT2

To investigate the function of bcSTAT2 in IFN signaling pathway,

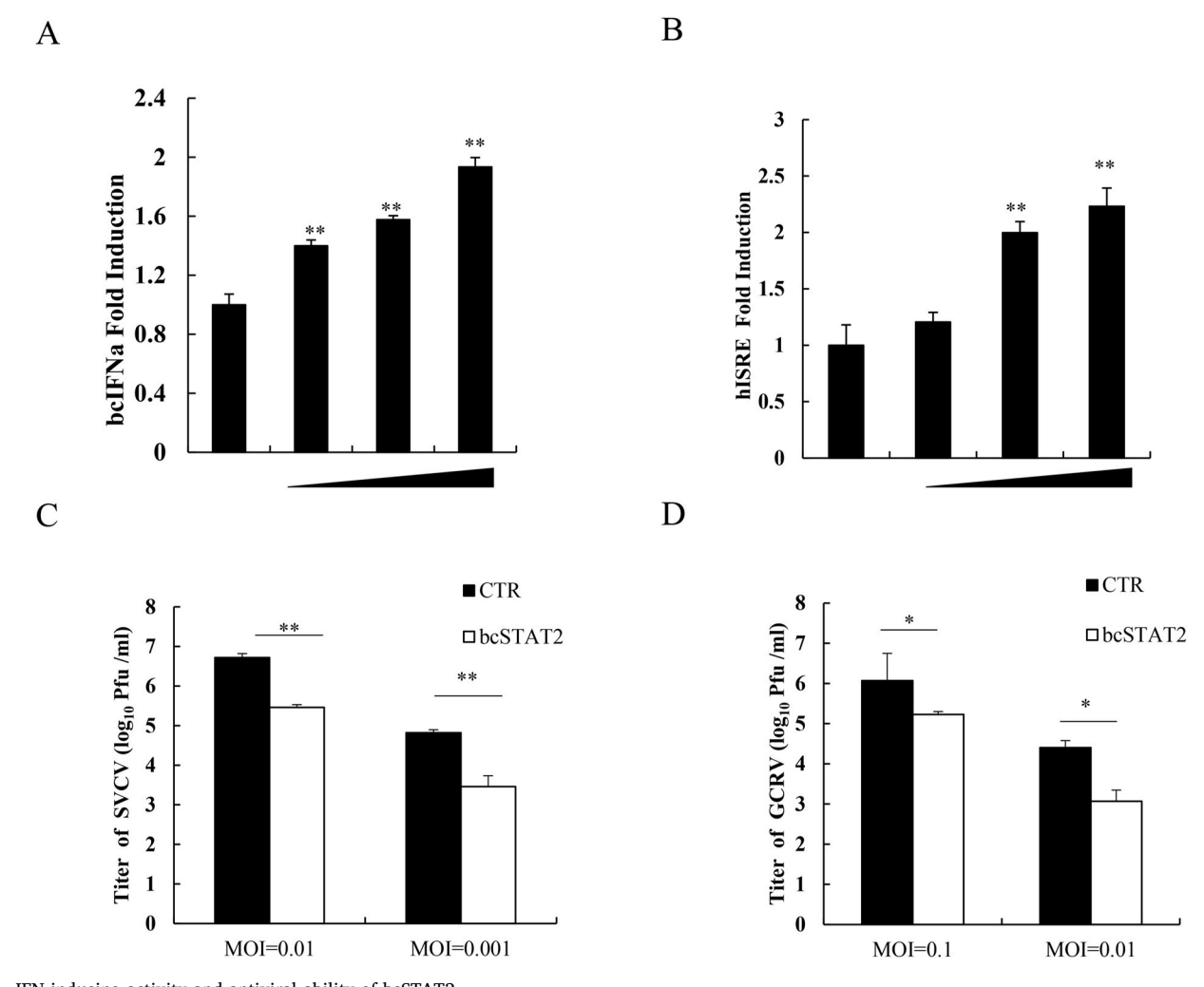


Fig. 4. IFN-inducing activity and antiviral ability of bcSTAT2 (A–B): EPC cells in 24-well plate (4×10^5 cells/well) were co-transfected with pRL-TK (25 ng), and bcSTAT2 (50ng/100ng/200 ng), Luci-bcIFNa (200 ng) (A) or Luci-hISRE (200 ng) (B). The transcription level of bcIFNa or hISRE promoter induced by bcSTAT2 was determined by the dual-luciferase reporter assay. The total amount of plasmid DNA was balanced by the empty vector (pcDNA5/FRT/TO). (C–D): EPC cells in 24-well plate (4×10^5 cells/well) were transfected with the plasmids expressing bcSTAT2 or the empty vector (400 ng), and infected with SVCV(C) or GCRV(D) at 24 hpt. The supernatant was collected and applied to the plaque assay. CTR: pcDNA5/FRT/TO; bcSTAT2: pcDNA5/FRT/TO-bcSTAT2-Myc.

EPC cells were transfected with the plasmid expressing bcSTAT2 and used for the dual-luciferase reporter assay. The transcription of bcIFNa and hISRE promoters was slightly up-regulated by bcSTAT2 (Fig. 4A&B). To further explore the role of bcSTAT2 in the antiviral innate immunity, EPC cells were transfected with the plasmid expressing bcSTAT2 or the empty vector respectively, and infected with GCRV or SVCV at 24 hpt. The viral titers of the supernatant media were examined by the plaque assay, in which the viral titers of the cells transfected with bcSTAT2 were lower than that of control (Fig. 4C&D). Our data demonstrated that black carp STAT2 functions importantly during the antiviral innate immune response.

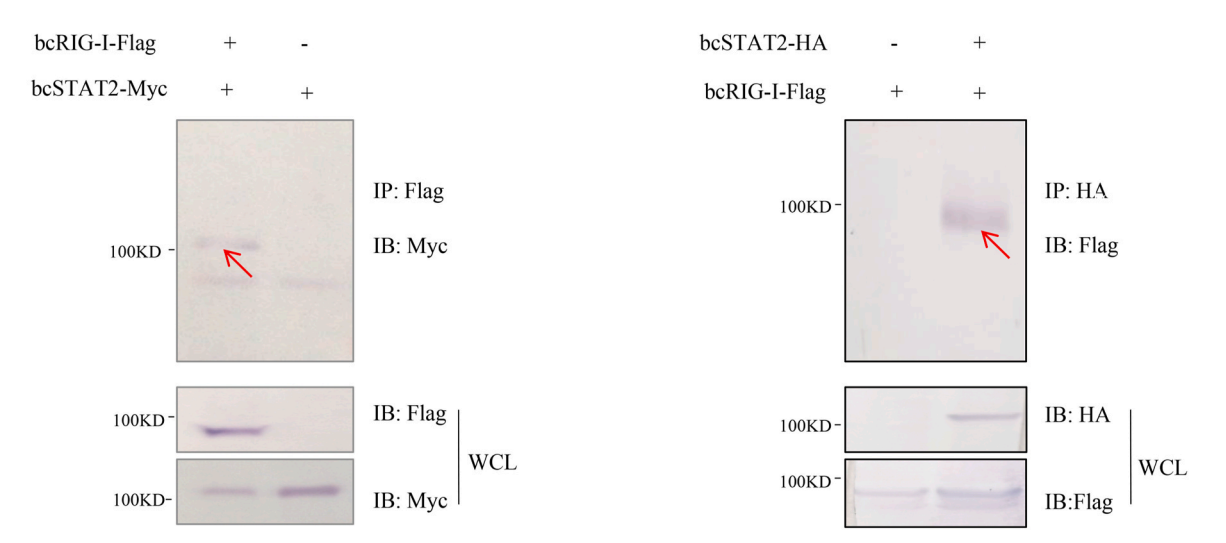
3.5. The interaction between bcSTAT2 and bcRIG-I

In mammals, STAT4, a member of the STAT family, has been found to promote RIG-I-triggered type I IFNs production in response to RNA virus infection [25]. Meanwhile, to our knowledge, there are no reports on PRRs regulation by STAT family members in teleost. To investigate the relationship between bcSTAT2 and bcRIG-I, HEK293T cells were co-transfected with bcSTAT2 and bcRIG-I, and used for co-IP assay. The specific band of \sim 106 kDa (red arrow indicated) representing bcSTAT2 was detected in the bcRIG-I-precipitated proteins (Fig. 5A). Similarly,

the specific band of \sim 96 kDa (red arrow indicated) of bcRIG-I was detected in the bcSTAT2-precipitated proteins (Fig. 5B). Thus, these results collectively demonstrated that bcSAT2 interacts with bcRIG-I.

3.6. bcSTAT2 down-regulated bcRIG-I-mediated IFN transcription

To investigate the role of bcSTAT2 in the regulation of bcRIG-I mediated IFN signaling pathway, EPC cells were transfected with plasmids expressing bcSTAT2 and/or bcRIG-I separately. The cells were harvested at 24 hpt and used for dual-luciferase reporter assay. The result clearly indicated that bcSTAT2 strongly inhibited bcRIG-I-induced the transcription of DrIFNφ3 (Fig. 6A), bcIFNa (Fig. 6B) and eIFN (Fig. 6C) promoter in a dose-dependent manner. In mammals, the Nterminal CARD domain of RIG-I is crucial for activating downstream signaling transduction [36,37]. To further explore whether bcSTAT2 functions on CARDs to suppress bcRIG-I mediated IFN signaling. We co-transfected the plasmid expressing bcSTAT2 and/or bcRIG-I-CARD into EPC cells, the result of dual-luciferase reporter assay showed that the transcription levels of DrIFNφ3 (Fig. 6D), bcIFNa (Fig. 6E) and eIFN (Fig. 6F) promoter induced by bcRIG-I-CARD were significantly reduced by bcSTAT2. These results suggested that bcSTAT2 straightforwardly suppressed bcRIG-I-CARD mediated IFN signaling pathway.



B

Fig. 5. The interaction between bcSTAT2 and bcRIG-I (A- B) HEK293T cells in 100 mm plate were transfected with bcSTAT2 (7.5 μg) and/or bcRIG-I (7.5 μg), 48 h after transfection, the cells were harvested for the co-IP assay. IP: immunoprecipitation; WCL: whole cell lysate. bcRIG-I-Flag: pcDNA5/FRT/TO-bcRIG-I-Flag; bcSTAT2-Myc: pcDNA5/FRT/TO-bcSTAT2-HA: pcDNA5/FRT/TO-bcSTAT2-HA.

3.7. bcSTAT2 dampened bcRIG-I-mediated antiviral activity

Our previous study had reported that bcRIG-I owns strong antiviral ability against SVCV and GCRV [33]. To investigate the effect of bcSTAT2 on bcRIG-I mediated antiviral signaling pathway. EPC cells co-expressing bcSTAT2 or/and bcRIG-I were infected with SVCV with different MOIs (0.01 or 0.1) at 24 hpt. Then the supernatant was collected for the plaque assay, and the cells pellets was used for qRT-PCR. The plaque assay showed that the viral titer of the cells co-transfected with bcRIG-I and bcSTAT2 were much higher than those of the cells transfected with bcRIG-I (Fig. 7A). Simultaneously, the mRNA levels of SVCV genes, including SVCV-G, SVCV-P and SVCV-M, in the cells co-expressing bcRIG-I and bcSTAT2 were much higher than those of the cells expressing bcRIG-I alone (Fig. 7B). These above data corporately showed that bcSTAT2 functions as a negative regulator in bcRIG-I regulation during the antiviral innate immune response.

3.8. bcSTAT2 impaired K63-linked ubiquitination of bcRIG-I

In mammals, the formation of oligomer and K63-linked ubiquitination are essential for RIG-I activation [38-40]. To delineate the molecular mechanism behind the regulation of bcRIG-I by bcSTAT2, the SDD-AGE assay was applied to test whether the oligomerization of bcRIG-I was affected by bcSTAT2 or not. Our result demonstrated that the oligomerization of bcRIG-I was not affected by bcSTAT2 (Fig. 8A). Next, we investigated whether bcSTAT2 was involved in the ubiquitination of bcRIG-I. HEK293T cells were co-transfected with HA-Ub, bcRIG-I and/or bcSTAT2, and bcRIG-I protein were precipitated separately to examine its ubiquitination. As shown in Fig. 8B, compared with the group that bcRIG-I was transfected alone, bcSTAT2 significantly reduced the ubiquitination of bcRIG-I in the group co-transfected with bcSTAT2 and bcRIG-I. To further examine which type of polyubiquitin chains on bcRIG-I was regulated by bcSTAT2, HA-Ub-K48O and HA-Ub-K63O were recruited in the above assay separately. The K63-linked ubiquitination of bcRIG-I was obviously attenuated by bcSTAT2; conversely, the K48-linked ubiquitination of bcRIG-I in the co-transfection group was similar to that of bcRIG-I transfection alone group (Fig. 8C). This result demonstrated that bcSTAT2 negatively regulated the bcRIG-I-mediated IFN signaling pathway by dampening the K63-linked polyubiquitination of bcRIG-I.

3.9. Diagram the functional domain of bcSTAT2 in bcRIG-I regulation

bcSTAT2 contains the same functional domains to those of its mammalian counterparts, including a ND, a CCD, a DBD, a LD, a SH2 and a TAD. To identify the role of the domains of bcSTAT2 in bcRIG-I regulation, we constructed six different truncation mutants: bcSTAT2-△ND (truncation mutant lacking N-terminal domain), bcSTAT2-△CCD (coiled-coil domain deleted), bcSTAT2-\DBD (DNA-binding domain deleted), bcSTAT2-△LD (linker domain deleted), bcSTAT2-△SH2 (Src homology 2 domain deleted) and bcSTAT2-\transactivation domain deleted) (Fig. 9A). EPC cells were transfected with the truncation mutants respectively, and subjected to the IB assay. The result showed that all truncation mutants were well-expressed in EPC cells (Fig. 9B). Then, EPC cells were co-transfected with bcRIG-I and bcSTAT2 or its truncation mutants, and the transcription activity of bcIFNa and eIFN promoter was examined by dual-luciferase reporter assay. The result revealed that the bcSTAT2-△SH2 and bcSTAT2-△TAD mutants significantly suppressed bcRIG-I mediated IFN promoter transcription, just like wild-type bcSTAT2. In contrast, the bcSTAT2-△CCD mutant lost the inhibitory effects on bcRIG-I-mediated IFN promoter transcription (Fig. 9C). Therefore, we concluded that the CCD domain of bcSTAT2 is indispensable for its negative regulation of bcRIG-I.

4. Discussion

IFN production is crucial for both innate immunity and adaptive immunity. However, an excessive immune response leads to the tissue damage and autoimmune diseases. Therefore, IFN activation and signaling pathways must be strictly regulated to maintain immune homeostasis [41]. RIG-I, as a key cytoplasmic PRR, recognizes intracellular viral RNA and activates downstream IFN regulatory factors (IRFs) and NF-kB, thereby inducing the production of type I IFNs and inflammatory factors, and eliminating invading virus [37]. Thus, the regulatory

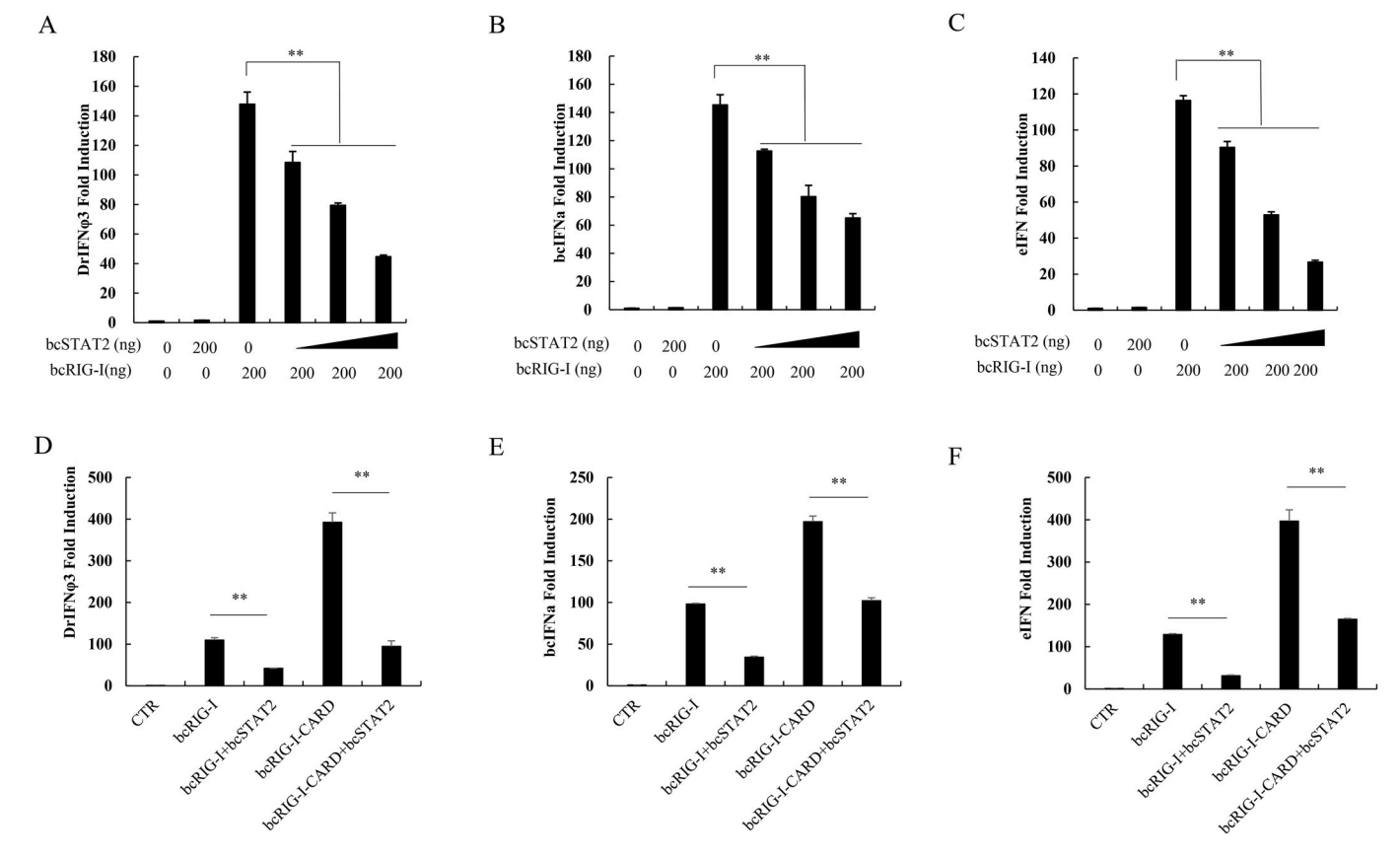


Fig. 6. bcSTAT2 dampened bcRIG-I mediated IFN signaling (A- C) The plasmids expressing bcRIG-I (200 ng), bcSTAT2 (50ng/100ng/200 ng) and pRL-TK (25 ng), Luci-DrIFN ϕ 3 (200 ng) (A), Luci-bcIFNa (200 ng) (B) or Luci-eIFN (200 ng) (C) were co-transfected into EPC cells in 24-well plate (4 × 10⁵ cells/well) respectively. The cells were harvested at 24 hpt and subjected to the dual-luciferase reporter assay. (D–F) EPC cells in 24-well plate (4 × 10⁵ cells/well) were co-transfected with the plasmids expressing bcRIG-I-CARD mutant (100 ng), bcSTAT2 (50ng/100ng/200 ng), pRL-TK (25 ng), Luci-DrIFN ϕ 3 (200 ng) (D), Luci-bcIFNa (200 ng) (E) or Luci-eIFN (200 ng) (F) respectively, and applied to the dual-luciferase reporter assay separately. CTR: pcDNA5/FRT/TO-bcRIG-I-Flag; bcSTAT2: pcDNA5/FRT/TO/-bcSTAT2-Myc; bcRIG-I-CARD: pcDNA5/FRT/TO-bcRIG-I-CARD-Flag.

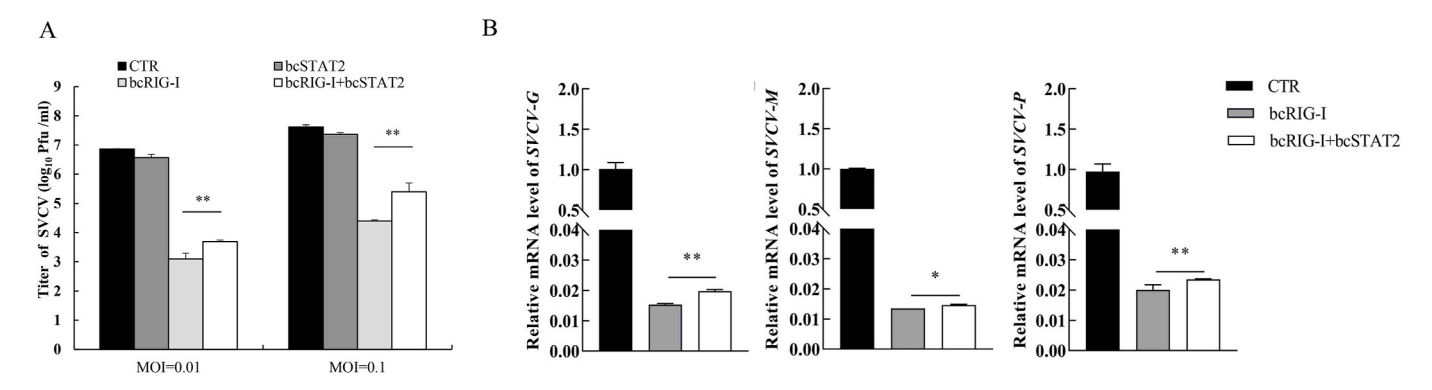


Fig. 7. bcSTAT2 inhibited bcRIG-I-mediated antiviral activity (A) EPC cells in 24-well plate (4×10^5 cells/well) were transfected with bcRIG-I (200 ng) and/or bcSTAT2 (200 ng), and infected with SVCV at 24 hpt. The supernatant was collected for the plaque assay. (B) EPC cells in 6-well plate (2×10^6 cells/well) were co-transfected with bcRIG-I ($1.5 \mu g$) and/or bcSTAT2 ($1.5 \mu g$) separately, and infected with SVCV (MOI = 0.1) at 24 hpt. The cells were harvested and relative mRNA level of *SVCV-G*, *SVCV-M*, *SVCV-P* was detected by the qRT-PCR. CTR: pcDNA5/FRT/TO; bcRIG-I: pcDNA5/FRT/TO-bcRIG-I-Flag; bcSTAT2:pcDNA5/FRT/TO/-bcSTAT2-Myc.

mechanisms of RIG-I have been extensively studied. In resting time, RIG-I is kept an autoinhibition state via the internal interaction between N-terminal CARD domain and the intermediate helicase domain, preventing premature signaling before infection [26]. Meanwhile, RIG-I can also be positively or negatively modulated by post-translational modification, such as phosphorylation, ubiquitination and acetylation. In particularly, ubiquitination is very important for regulating the

activation of RIG-I. The C-terminal SPRY domain of TRIM25 interacts with the first N-terminal CARD domain of RIG-I, which effectively delivers the K63-linked ubiquitin to the second CARD domain, resulting in the activation of RIG-I mediated signaling pathway [38]. Meanwhile, positive regulators such as E3 ubiquitin ligases RNF135, TRIM4 and MEX3C have also been shown to mediate the K63-linked ubiquitination of RIG-I, thereby promoting RIG-I mediated signaling [42–44]. In

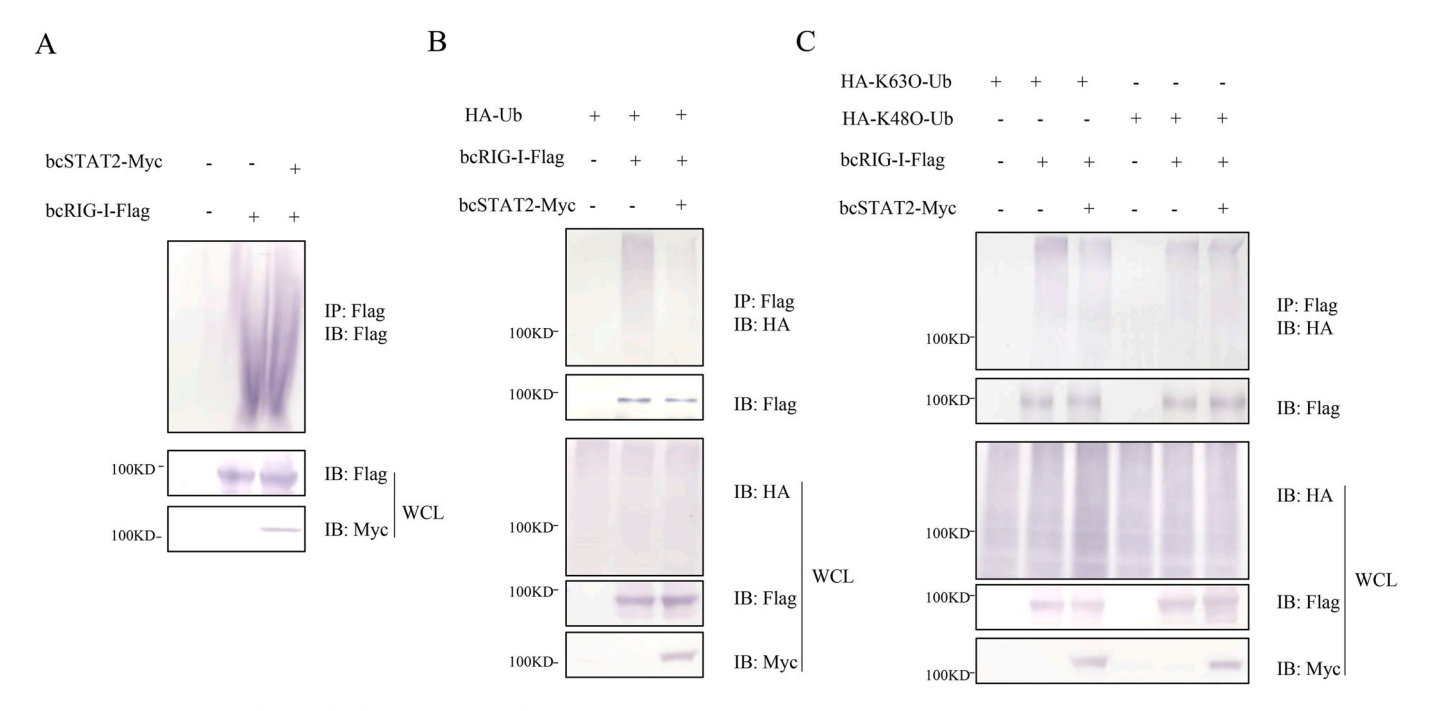


Fig. 8. bcSTAT2 suppressed K63-linked ubiquitination of bcRIG-I

(A) HEK293T cells in 100 mm plate were transfected with bcRIG-I (7.5 µg) and/or bcSTAT2 (7.5 µg) separately, and were harvested at 48 hpt for the SDD-AGE assay. (B&C) HEK293T cells in 100 mm plate were co-transfected with HA-Ub (HA-Ub-K63O or HA-Ub-K48O) (5 µg), bcSTAT2 (5 µg) and/or bcRIG-I (5 µg) respectively. The transfected cells were harvested for co-IP at 48 hpt. SDD-AGE: semi-denaturing detergent agarose gel electrophoresis. bcRIG-I-Flag; pcDNA5/FRT/TO-bcRIG-I-Flag; bcSTAT2-Myc; pcDNA5/FRT/TO-bcSTAT2-Myc; HA-Ub: pcDNA5/FRT/TO-HA-Ub; HA-Ub-K63O: pcDNA5/FRT/TO-HA-Ub-K63O; HA-Ub-K48O: pcDNA5/FRT/TO-HA-Ub-K48O.

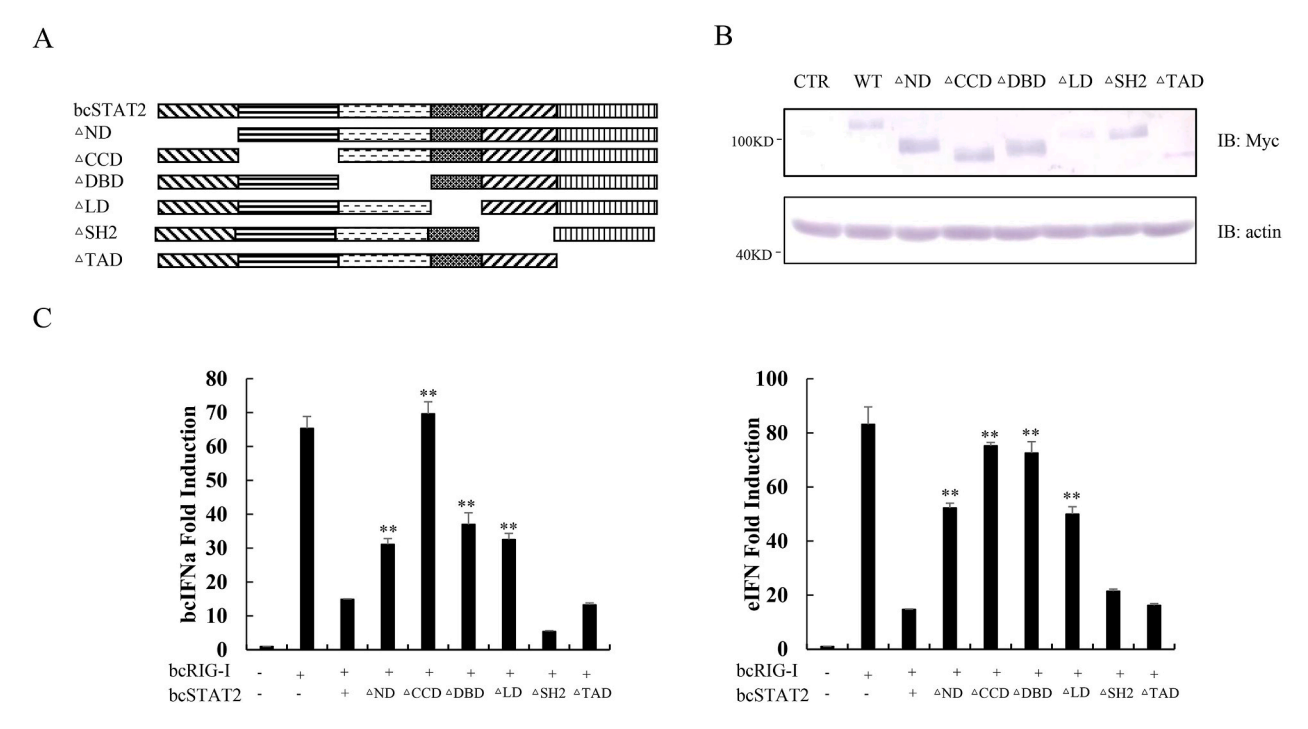


Fig. 9. The functional domain of bcSTAT2 in bcRIG-I regulation (A) Schematic diagram of the domain of bcSTAT2 and its truncation mutants. (B) EPC cells in 6-well plate (2×10^6 cells/well) were transfected with bcSTAT2 or the indicated truncation mutants (3 μ g), respectively. The protein expression was detected by IB assay at 48 hpt. (C) EPC cells in 24-well plate (4×10^5 cells/well) were co-transfected with pRL-TK (25 ng), Luci-bcIFNa (200 ng) or Luci-eIFN (200 ng), bcRIG-I (100 ng) and/or bcSTAT2 (truncation mutants of bcSTAT2) (200 ng). The cells were harvested at 24 hpt and used for reporter assay. bcRIG-I: pcDNA5/FRT/TO-bcRIG-I-Flag; bcSTAT2: pcDNA5/FRT/TO-bcSTAT2-Myc; \triangle ND: pcDNA5/FRT/TO/-bcSTAT2- \triangle DBD-Myc; \triangle CD: pcDNA5/FRT/TO/-bcSTAT2- \triangle DBD-Myc; \triangle LD: pcDNA5/FRT/TO/-bcSTAT2- \triangle LD-Myc; \triangle SH2: pcDNA5/FRT/TO/- bcSTAT2- \triangle TAD: pcDNA5/FRT/TO/-bcSTAT2- \triangle TAD-Myc.

contrast, deubiquitinating enzymes such as CYLD, USP21 and USP3 negatively regulate RIG-I/IFN signaling by removing the K63-linked polyubiquitination chain [45-47]. In this study, we showed that STAT2, originally identified as the downstream factor of IFN, inhibited RIG-I mediated antiviral innate immune response by reducing the K63-linked ubiquitination of RIG-I in black carp. Before that, researchers have found that cytoplasmic STAT4 interacts with E3 ligase CHIP, which leads to the proteasomal degradation of RIG-I by K48-linked ubiquitination, and promotes type I IFNs production [25]. Moreover, we found that the transcription level of bcSTAT2 was improved in the early stage of GCRV and SVCV infection, and reached the maximum at 12 hpi and 24 hpi, respectively. While the transcription level of bcSTAT2 was decreased at 48 hpi (Fig. 2B&C). Therefore, we hypothesized that bcSTAT2 is involved in the antiviral immune system in the early stage of viral infection, inducing the production of downstream ISGs, thereby protecting host cells from viral infection. Whereas, bcSTAT2 might bind to bcRIG-I in the later stages of viral infection to prevent the overactivation of signaling pathway and maintain immune homeostasis.

In mammals, STAT2 forms ISGF3 complex with STAT1 and IRF9, which is responsible for the induction of ISGs [48,49]. However, STAT2 has been reported as a negative regulator of innate immune responses in mammals. USP18 recruits STAT2 to exhibit its inhibitory effect on IFN signaling [50]. Simultaneously, STAT2 has also been found to negatively regulate STING, leading to the suppression of cGAMP-induced expression of IRF-dependent genes [51]. In the present study, we revealed that STAT2 interacted with RIG-I (Fig. 5), and restrained the IFN promoter expression and the antiviral ability induced by RIG-I (Figs. 6 and 7). Similarly to its mammalian counterpart, bcSTAT2 contains ND, CCD, DBD, LD, SH2 and TAD (Fig. 1A). In mammals, STAT2 binds to STAT1 through its SH2 domain, and to IRF9 through its CC domain [52]. Nevertheless, we demonstrated that the bcSTAT2-△CCD mutant lost the ability to negatively regulate bcRIG-I mediated IFN expression (Fig. 9C). Therefore, we speculated that in order to prevent overactivation of bcRIG-I, bcSTAT2 competitively binds to bcRIG-I but not IRF9 through the CC domain, thus terminating signaling transduction. On the other hand, this interaction between bcRIG-I and bcSTAT2 attenuates the K63-linked ubiquitination of bcRIG-I, inhibiting bcRIG-I mediated IFN signaling pathway.

CRediT authorship contribution statement

Ji Liu: and. Chushan Dai: play the roles of investigation and original draft writing. Lijun Yin: and. Xiao Yang: and. Jun Yan: play the roles of investigation and formal analysis. Meiling Liu: and. Hui Wu: and. Jun Xiao: and. Weiguang Kong: contribute to data curation, Formal analysis, and writing. Zhen Xu: play the role of project administration and data curation. Hao Feng: contributes to, Conceptualization, Formal analysis, Project administration, and writing.

Declaration of competing interest

The authors declare that the research was conducted in the absence of any commercial or financial relationships that could be construed as a potential conflict of interest.

Data availability

Data will be made available on request.

Acknowledgements

This work was supported by the National Natural Science Foundation of China (31920103016, U21A20268, U22A20535, UA23A20252, 32303050), Hunan Provincial Science and Technology Department (2022JJ40271, 2023JJ40435), Postgraduate Scientific Research Innovation Project of Hunan Province (QL20210135), the earmarked fund

for Hunan Agriculture Research System, the Research and Development Platform of Fish Disease and Vaccine for Postgraduates in Hunan Province.

Appendix A. Supplementary data

Supplementary data to this article can be found online at https://doi.org/10.1016/j.fsi.2024.109510.

References

- F. McNab, K. Mayer-Barber, A. Sher, A. Wack, A. O'Garra, Type I interferons in infectious disease, Nat. Rev. Immunol. 15 (2) (2015) 87–103.
- [2] A. García-Sastre, Ten strategies of interferon evasion by viruses, Cell Host Microbe 22 (2) (2017) 176–184.
- [3] O. Takeuchi, S. Akira, Pattern recognition receptors and inflammation, Cell 140 (6) (2010) 805–820.
- [4] J. Liu, S.X. Liu, X.T. Cao, Highlights of the advances in basic immunology in 2011, Cell. Mol. Immunol. 9 (3) (2012) 197–207.
- [5] E. Meylan, J. Tschopp, M. Karin, Intracellular pattern recognition receptors in the host response, Nature 442 (7098) (2006) 39–44.
- [6] N. Yan, Z.J. Chen, Intrinsic antiviral immunity, Nat. Immunol. 13 (3) (2012)
- [7] S. Pestka, C.D. Krause, M.R. Walter, Interferons, interferon-like cytokines, and their receptors, Immunol. Rev. 202 (2004) 8–32.
- [8] G.R. Stark, J.E. Darnell Jr., The JAK-STAT pathway at twenty, Immunity 36 (4) (2012) 503–514.
- [9] J.N. Ihle, The Stat family in cytokine signaling, Curr. Opin. Cell Biol. 13 (2) (2001) 211–217.
- [10] P. Xin, X.Y. Xu, C.J. Deng, S. Liu, Y.Z. Wang, X.G. Zhou, H.X. Ma, D.H. Wei, S. Q. Sun, The role of JAK/STAT signaling pathway and its inhibitors in diseases, Int. Immunopharm. 80 (2020) 106210.
- [11] S.S. Liu, Y. Liao, B. Chen, Y.H. Chen, Z.D. Yu, H.T. Wei, L.F. Zhang, S.L. Huang, P. B. Rothman, G.F. Gao, J.L. Chen, Critical role of Syk-dependent STAT1 activation in innate antiviral immunity, Cell Rep. 34 (3) (2021) 108627.
- [12] X.Y. Fu, D.S. Kessler, S.A. Veals, D.E. Levy, J.E. Darnell Jr., ISGF3, the transcriptional activator induced by interferon alpha, consists of multiple interacting polypeptide chains, Proc. Natl. Acad. Sci. U.S.A. 87 (21) (1990) 8555–8559.
- [13] Y. Zhang, Y.L. Chen, H.L. Yun, Z.Y. Liu, M. Su, R. Lai, STAT1β enhances STAT1 function by protecting STAT1α from degradation in esophageal squamous cell carcinoma, Cell Death Dis. 8 (10) (2017) e3077.
- [14] M.A. Meraz, J.M. White, K.C. Sheehan, E.A. Bach, S.J. Rodig, A.S. Dighe, D. H. Kaplan, J.K. Riley, A.C. Greenlund, D. Campbell, K. Carver-Moore, R.N. DuBois, R. Clark, M. Aguet, R.D. Schreiber, Targeted disruption of the Stat1 gene in mice reveals unexpected physiologic specificity in the JAK-STAT signaling pathway, 1996 Feb 9, Cell 84 (3) (1996) 431–442.
- [15] A. García-Sastre, R.K. Durbin, H. Zheng, P. Palese, R. Gertner, D.E. Levy, J. E. Durbin, The role of interferon in influenza virus tissue tropism, J. Virol. 72 (11) (1998) 8550–8558.
- [16] T.J. Pasieka, B. Lu, D.A. Leib, Enhanced pathogenesis of an attenuated herpes simplex virus for mice lacking Stat1, J. Virol. 82 (12) (2008) 6052–6055.
- [17] C. Park, S. Li, E. Cha, C. Schindler, Immune response in Stat2 knockout mice, Immunity 13 (6) (2000) 795–804.
- [18] S.T. Perry, M.D. Buck, S.M. Lada, C. Schindler, S. Shresta, STAT2 mediates innate immunity to Dengue virus in the absence of STAT1 via the type I interferon receptor, PLoS Pathog. 7 (2) (2011) e1001297.
- [19] S. Hambleton, S. Goodbourn, D.F. Young, P. Dickinson, M.B. Mohamad, M. Valappil, N. McGovern, A.J. Cant, S.J. Hackett, P. Ghazal, N.V. Morgan, R. E. Randall, STAT2 deficiency and susceptibility to viral illness in humans, Proc. Natl. Acad. Sci. U.S.A. 110 (8) (2013) 3053–3058.
- [20] C.Y. Yue, J. Xu, M.D. Tan Estioko, K.P. Kotredes, Y. Lopez-Otalora, B.A. Hilliard, D. P. Baker, S. Gallucci, A.M. Gamero, Host STAT2/type I interferon axis controls tumor growth, Int. J. Cancer 136 (1) (2015) 117–126.
- [21] J.P. Wang, N. Pham-Mitchell, C. Schindler, I.L. Campbell, Dysregulated Sonic hedgehog signaling and medulloblastoma consequent to IFN-alpha-stimulated STAT2-independent production of IFN-gamma in the brain, J. Clin. Invest. 112 (4) (2003) 535–543
- [22] Y.H. Qin, H.X. Liu, P.P. Zhang, S. Deng, R. Qiu, L.G. Yao, Molecular cloning, expression and functional analysis of STAT2 in orange-spotted grouper, Epinephelus coioides, Fish Shellfish Immunol. 131 (2022) 1245–1254.
- [23] N. Wang, X.L. Wang, C.G. Yang, S.L. Chen, Molecular cloning, subcellular location and expression profile of signal transducer and activator of transcription 2 (STAT2) from turbot, Scophthalmus maximus, Fish Shellfish Immunol. 35 (4) (2013) 1200–1208.
- [24] S.D.N.K. Bathige, N. Umasuthan, T.T. Priyathilaka, W.S. Thulasitha, J.D.H. E. Jayasinghe, Q. Wan, B.H. Nam, J. Lee, Molecular cloning, transcriptional profiling, and subcellular localization of signal transducer and activator of transcription 2 (STAT2) ortholog from rock bream, *Oplegnathus fasciatus*, Gene 626 (2017) 95–105.
- [25] K. Zhao, Q. Zhang, X. Li, D.Z. Zhao, Y.Q. Liu, Q.C. Shen, M.J. Yang, C.M. Wang, N. Li, X.T. Cao, Cytoplasmic STAT4 promotes antiviral type I IFN production by

- blocking CHIP-mediated degradation of RIG-I, J. Immunol. 196 (3) (2016) 1209–1217
- [26] D. Kolakofsky, E. Kowalinski, S. Cusack, A structure-based model of RIG-I activation, RNA 18 (12) (2012) 2118–2127.
- [27] D.W. Leung, G.K. Amarasinghe, Structural insights into RNA recognition and activation of RIG-I-like receptors, Curr. Opin. Struct. Biol. 22 (3) (2012) 297–303.
- [28] K.H. Kok, P.Y. Lui, M.H. James Ng, K.L. Siu, S.W. Ngor Au, D.Y. Jin, The double-stranded RNA-binding protein PACT functions as a cellular activator of RIG-I to facilitate innate antiviral response, Cell Host Microbe 9 (4) (2011) 299–309.
- [29] Z.Y. Liu, C. Wu, Y.Y. Pan, H. Liu, X.M. Wang, Y.T. Yang, M.D. Gu, Y.Y. Zhang, X. J. Wang, NDR2 promotes the antiviral immune response via facilitating TRIM25-mediated RIG-I activation in macrophages, Sci. Adv. 5 (2) (2019) eaav0163.
- [30] S.T. Chen, L. Chen, D.S. Lin, S.Y. Chen, Y.P. Tsao, H.T. Guo, F.J. Li, W.T. Tseng, J. W. Tam, C.W. Chao, W.J. Brickey, I. Dzhagalov, M.J. Song, H.R. Kang, J.U. Jung, J. P. Ting, NLRP12 regulates anti-viral RIG-I activation via interaction with TRIM25, Cell Host Microbe 25 (4) (2019) 602–616.
- [31] Y.X. He, J. Liu, Y.J. Miao, M.L. Liu, H. Wu, J. Xiao, H. Feng, Black carp LGP2 suppresses RIG-I mediated IFN signaling during the antiviral innate immunity, Fish Shellfish Immunol. 143 (2023) 109208.
- [32] Y.L. Rao, Q.Y. Wan, C.R. Yang, J.G. Su, Grass carp laboratory of genetics and physiology 2 serves as a negative regulator in retinoic acid-inducible gene I- and melanoma differentiation-associated gene 5-mediated antiviral signaling in resting state and early stage of grass carp reovirus infection, Front. Immunol. 8 (2017) 352
- [33] J. Liu, Y.X. He, Y.J. Miao, C.S. Dai, J. Yan, M.L. Liu, J. Zou, H. Feng, The phenylalanine-28 is crucial for black carp RIG-I mediated antiviral signaling, Dev. Comp. Immunol. 148 (2023) 104917.
- [34] H. Wu, Y.Y. Zhang, X.Y. Lu, J. Xiao, P.H. Feng, H. Feng, STAT1a and STAT1b of black carp play important roles in the innate immune defense against GCRV, Fish Shellfish Immunol. 87 (2019) 386–394.
- [35] F.J. Hou, L.J. Sun, H. Zheng, B. Skaug, Q.X. Jiang, Z.J. Chen, MAVS forms functional prion-like aggregates to activate and propagate antiviral innate immune response, Cell 146 (3) (2011) 448–461.
- [36] D. Thoresen, W.S. Wang, D. Galls, R. Guo, L. Xu, A.M. Pyle, The molecular mechanism of RIG-I activation and signaling, Immunol. Rev. 304 (1) (2021) 154-168
- [37] M. Yoneyama, M. Kikuchi, T. Natsukawa, N. Shinobu, T. Imaizumi, M. Miyagishi, K. Taira, S. Akira, T. Fujita, The RNA helicase RIG-I has an essential function in double-stranded RNA-induced innate antiviral responses, Nat. Immunol. 5 (7) (2004) 730–737.
- [38] M.U. Gack, Y.C. Shin, C.H. Joo, T. Urano, C.Y. Liang, L.J. Sun, O. Takeuchi, S. Akira, Z.J. Chen, S. Inoue, J.U. Jung, TRIM25 RING-finger E3 ubiquitin ligase is essential for RIG-I-mediated antiviral activity, Nature 446 (7138) (2007) 916–920.
- [39] M.U. Gack, A. Kirchhofer, Y.C. Shin, K. Inn, C.Y. Liang, S. Cui, S. Myong, T. Ha, K. Hopfner, J.U. Jung, Roles of RIG-I N-terminal tandem CARD and splice variant

- in TRIM25-mediated antiviral signal transduction, Proc. Natl. Acad. Sci. U.S.A. 105 (43) (2008) 16743–16748.
- [40] J.R. Patel, A. García-Sastre, Activation and regulation of pathogen sensor RIG-I, Cytokine Growth Factor Rev. 25 (5) (2014) 513–523.
- [41] P.P. Hou, K.X. Yang, P.H. Jia, L. Liu, Y.X. Lin, Z.B. Li, J. Li, S.L. Chen, S.T. Guo, J. A. Pan, J.Y. Wu, H. Peng, W.J. Zeng, C.M. Li, Y.F. Liu, D.Y. Guo, +A novel selective autophagy receptor, CCDC50, delivers K63 polyubiquitination-activated RIG-I/MDA5 for degradation during viral infection, Cell Res. 31 (1) (2021) 62–79.
- [42] H. Oshiumi, M. Miyashita, N. Inoue, M. Okabe, M. Matsumoto, T. Seya, The ubiquitin ligase Riplet is essential for RIG-I-dependent innate immune responses to RNA virus infection, Cell Host Microbe 8 (6) (2010) 496–509.
- [43] J. Yan, Q. Li, A.P. Mao, M.M. Hu, H.B. Shu, TRIM4 modulates type I interferon induction and cellular antiviral response by targeting RIG-I for K63-linked ubiquitination, J. Mol. Cell Biol. 6 (2) (2014) 154–163.
- [44] K. Kuniyoshi, O. Takeuchi, S. Pandey, T. Satoh, H. Iwasaki, S. Akira, T. Kawai, Pivotal role of RNA-binding E3 ubiquitin ligase MEX3C in RIG-I-mediated antiviral innate immunity, Proc. Natl. Acad. Sci. U.S.A. 111 (15) (2014) 5646–5651.
- [45] C.S. Friedman, M.A. O'Donnell, D. Legarda-Addison, A. Ng, W.B. Cárdenas, J. S. Yount, T.M. Moran, C.F. Basler, A. Komuro, C.M. Horvath, R. Xavier, A.T. Ting, The tumour suppressor CYLD is a negative regulator of RIG-I-mediated antiviral response, EMBO Rep. 9 (9) (2008) 930–936.
- [46] Y.H. Fan, R.F. Mao, Y. Yu, S.F. Liu, Z.C. Shi, J. Cheng, H.Y. Zhang, L. An, Y.L. Zhao, X. Xu, Z.H. Chen, M. Kogiso, D. Zhang, H. Zhang, P.M. Zhang, J.U. Jung, X.N. Li, G. T. Xu, J.H. Yang, USP21 negatively regulates antiviral response by acting as a RIG-I deubiquitinase, J. Exp. Med. 211 (2) (2014) 313–328.
- [47] J. Cui, Y.X. Song, Y.Y. Li, Q.Y. Zhu, P. Tan, Y.F. Qin, H.Y. Wang, R.F. Wang, USP3 inhibits type I interferon signaling by deubiquitinating RIG-I-like receptors, Cell Res. 24 (4) (2014) 400–416.
- [48] S.V. Kotenko, G. Gallagher, V.V. Baurin, A. Lewis-Antes, M.L. Shen, N.K. Shah, J. A. Langer, F. Sheikh, H. Dickensheets, R.P. Donnelly, IFN-lambdas mediate antiviral protection through a distinct class II cytokine receptor complex, Nat. Immunol. 4 (1) (2003) 69–77.
- [49] M.M. Brierley, K.L. Marchington, I. Jurisica, E.N. Fish, Identification of GAS-dependent interferon-sensitive target genes whose transcription is STAT2-dependent but ISGF3-independent, FEBS J. 273 (7) (2006) 1569–1581.
- [50] K. Arimoto, S. Löchte, S.A. Stoner, C. Burkart, Y. Zhang, S. Miyauchi, S. Wilmes, J. Fan, J.J. Heinisch, Z. Li, M. Yan, S. Pellegrini, F. Colland, J. Piehler, D. Zhang, STAT2 is an essential adaptor in USP18-mediated suppression of type I interferon signaling, Nat. Struct. Mol. Biol. 24 (3) (2017) 279–289.
- [51] C.Y. Wang, J. Nan, E. Holvey-Bates, X. Chen, S. Wightman, M. Latif, J.J. Zhao, X. X. Li, G.C. Sen, G.R. Stark, Y.X. Wang, STAT2 hinders STING intracellular trafficking and reshapes its activation in response to DNA damage, Proc. Natl. Acad. Sci. U.S.A. 120 (16) (2023) e2216953120.
- [52] S. Rengachari, S. Groiss, J.M. Devos, E. Caron, N. Grandvaux, D. Panne, Structural basis of STAT2 recognition by IRF9 reveals molecular insights into ISGF3 function, Proc. Natl. Acad. Sci. U.S.A. 115 (4) (2018) E601–E609.